THE ROYAL SWEDISH ACADEMY OF SCIENCES

INSTITUT MITTAG-LEFFLER

Auravägen 17, SE-182 60 Djursholm, Sweden
Tel. +46 8 622 05 60 Fax. +46 8 622 05 89
info@mittag-leffler.se www.mittag-leffler.se

Investigations of the instability of Nariai asymptotics within the Gowdy class

F. Beyer

REPORT No. 31, 2008/2009, fall

ISSN 1103-467X
ISRN IML-R- -31-08/09- -SE+fall

Investigations of the instability of Nariai asymptotics within the Gowdy class

Florian Beyer
beyer@ann.jussieu.fr

Laboratoire Jacques-Louis Lions
Université Pierre et Marie Curie (Paris 6)
4 Place Jussieu, 75252 Paris, France

Abstract

In a previous paper, the author discussed that, according to the cosmic no-hair conjecture, the asymptotics of the generalized Nariai solutions should be non-generic among solutions of Einstein's field equations in vacuum with a positive cosmological constant. We proved that this is true within the class of spatially homogeneous solutions. In this paper now, we continue these investigations within the spatially inhomogeneous Gowdy case. For this, we use the numerical approach based on spectral methods, which the author discussed in another work. We are again able to confirm the non-genericity, describe some of the dynamics and show a new instability present here, which might yield another class of critical solutions.

1 Introduction

In this paper we are interested in a particular consequence of the cosmic no-hair conjecture. The fundamental question is the following: what are the properties of generic solutions of Einstein's field equations during an expanding phase? It is clear that this question is directly related to the problem of finding the correct interpretation of current cosmological observations because our universe seems to be at an epoch of its history in which it is expanding more and more rapidly. These observations are surprisingly consistent with spatially homogeneous and isotropic model solutions of Einstein's field equations with a positive cosmological constant [21, 22]. However, it is unclear how much these results depend on the high symmetry of the models. There are various approaches to study more general models. In any case, supposing that our universe is really isotropic and homogeneous and expands at an accelerated rate at present, it is natural to ask whether our universe is special with this property or if generic models undergoing such strong inflationary expansion phases become like this eventually. The conjecture that this behavior is generic for expanding cosmological solutions of Einstein's field equations in vacuum with a positive, cosmological constant

$$G_{\mu\nu} + \Lambda g_{\mu\nu} = 0, \tag{1}$$

is known as the "cosmic no-hair" conjecture which was essentially introduced in [14]. In the literature, this conjecture is often formulated for a wider class of models, but let us restrict to vacuum with $\Lambda > 0$ here. It states that, generically, such solutions will approach the de-Sitter solution asymptotically in the expanding phase in some way, and hence become more and more homogeneous and isotropic eventually. From this point of view, a particularly interesting solution of Eq. (1) is the so-called Nariai solution, which we introduce in Section 3. The late time asymptotics of this solution is extraordinary because the solution expands in an anisotropic manner into the future. If the cosmic no-hair conjecture is true, it implies that the asymptotics of the Nariai solution are instable in some sense.

We have started to investigate the question whether this is true in [5]. There, we introduced a generalized class of Nariai solutions and studied the question of genericity of Nariai asymptotics within the spatially homogeneous class as a first step. In this class the expected instability was confirmed. Namely for arbitrarily small spatially homogeneous perturbations of Nariai data, the corresponding solution either expands and forms a smooth conformal boundary consistent with the cosmic no-hair picture, or it collapses and forms a curvature singularity. The next natural step in these investigations would be to weaken the assumptions by considering the spherically symmetric case. Much is known about this case locally, for instance due to the "Birkhoff" theorem [24]. But to our knowledge there are no rigorous results of global nature which would be relevant for our investigations. There are several heuristic results as summarized in [6]. However, we have decided to proceed with the Gowdy symmetric case in this paper. We expect it to be difficult to handle this class analytically. One reason is the presence of symmetry axes. Indeed, there are several fundamental open problems in the class of Gowdy symmetric solutions with spatial $\mathbb{S}^1 \times \mathbb{S}^2$-topology, which are related to our interests here, for instance strong cosmic censorship [16, 12, 23]. Another motivation for studying this class is that we have already developed numerical techniques [4] for spatial $\mathbb{S}^3$-topology which can be applied to the $\mathbb{S}^1 \times \mathbb{S}^2$-Gowdy class, which is the relevant case here, as we describe below.

Let us list some of our main assumptions. We will always restrict our attention to cosmological solutions, by which we mean 4-dimensional globally hyperbolic solutions of Einstein's field equations in vacuum with a positive cosmological constant Λ and compact spatial topology. Spatial $\mathbb{S}^1 \times \mathbb{S}^2$-topology will be of particular interest for us, since this is the spatial topology of the Nariai solutions. We stress that we consider no quantum effects at all. When we speak of "perturbations of Nariai solutions", we always mean solutions of the fully non-linear Einstein equations, which are close to the Nariai solution in a sense we make clear later in this paper.

Our paper is organized as follows. In Section 3, we recall the properties of generalized Nariai solutions and summarize the results obtained in [5] for the spatially homogeneous case. In Section 4, we summarize basic facts about Gowdy symmetric spacetimes with spatial $\mathbb{S}^1 \times \mathbb{S}^2$-topology. In Section 5, we write a particular family of initial data for the field equations with the required properties. Section 6 is devoted to the discussion of our formulation of the field equations, our choice of gauge and our numerical techniques.

Finally in Section 7, we present our numerical results and interpret their meaning.

2 Notation and conventions

In this paper, we will always assume Einstein's summation convention to apply when we write tensorial expressions. Any tensor can be represented by the abstract symbol, say, T or by abstract index notation, e.g. $T^{\mu}{}_{\nu}$, depending on the context. Note, however, that when we write such an indexed object, we can mean either the abstract tensor or a special component with respect to some basis. Hopefully, this will always be clear from the context. Our convention is that Greek indices $\mu, \nu, \ldots = 0, \ldots, 3$ refer to some choice of local spacetime coordinates, whereas Latin indices $i, j, \ldots = 0, \ldots 3$ represent indices with respect to some orthonormal frame field. When we have chosen a time coordinate x^0, then Greek indices $\alpha, \beta, \ldots = 1, 2, 3$ represent spatial coordinates, and for a choice of frame $\{e_i\}$ with timelike vector field e_0, Latin indices $a, b, \ldots = 1, 2, 3$ refer to spatial frame indices. Writing $\{e_i\}$ just means the collection of tangent vector fields $\{e_0, \ldots, e_3\}$. If a 2-indexed object is written in brackets, for instance $(T^{\mu}{}_{\nu})$, we mean the matrix of its components, where the first index labels the lines of the matrix and the second one the columns.

3 Nariai solutions and spatially homogeneous perturbations

In [5], we discussed the class of generalized Nariai spacetimes. They are defined as the Lorentzian manifolds (M, g) with

$$M = I \times (\mathbb{S}^1 \times \mathbb{S}^2), \quad g = \frac{1}{\Lambda}\Big(-dt^2 + \underbrace{(\Phi_0 \cosh t + \Phi_0' \sinh t)}_{=:\Phi(t)}{}^2\, d\rho^2 + g_{\mathbb{S}^2}\Big),$$

for arbitrary $\Lambda > 0$, $\Phi_0 > 0$ and $\Phi_0' \in \mathbb{R}$. Here I is the unique maximal connected open interval in $\mathbb{R}$ such that $0 \in I$ and $\Phi|_I > 0$. All generalized Nariai spacetimes are analytic solutions of the vacuum Einstein's field equations with a cosmological constant Λ. They are globally hyperbolic and the $t = const$-hypersurfaces are spacelike Cauchy surfaces with topology $\mathbb{S}^1 \times \mathbb{S}^2$. Since the Cauchy surfaces are compact, the generalized Nariai spacetimes are cosmological solutions of Eq. (1). For $\Phi_0 = 1$ and $\Phi_0' = 0$, we speak of the standard Nariai spacetime (or solution) in order to stress that this is the Nariai spacetime which can be found in the literature, see for instance [6], and which was derived by Nariai in [17, 18]. All solutions are spatially homogeneous with Kantowski-Sachs symmetry group $G = \mathbb{R} \times \mathrm{SO}(3)$. The action of G can be represented, first, by translations along the $\mathbb{S}^1$-factor of the manifold generated by

$$\xi_3 = \partial_\rho, \tag{2a}$$

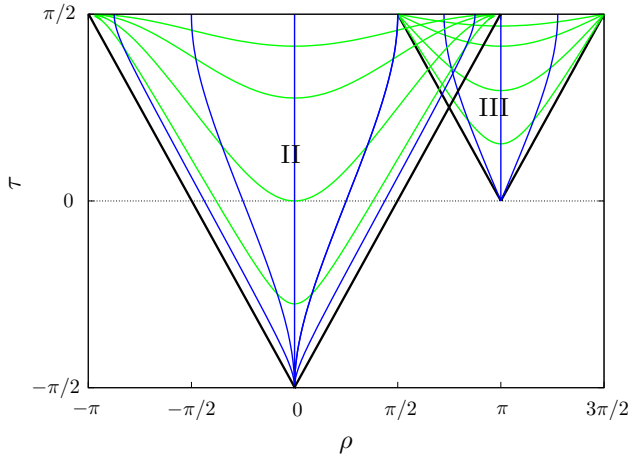

Fig. 1: Embeddings of generalized Nariai solutions into the standard one

corresponding to the $\mathbb{R}$-factor of G, and, second, by the standard action of SO(3) on $\mathbb{S}^2$, generated by

$$W_1 = \sin\phi\partial_\theta + \cos\phi\cot\theta\partial_\phi, \tag{2b}$$
$$W_2 = \cos\phi\partial_\theta - \sin\phi\cot\theta\partial_\phi, \tag{2c}$$
$$W_3 = \partial_\phi. \tag{2d}$$

Here (θ, ϕ) are standard polar coordinates on $\mathbb{S}^2$. However, the 4-dimensional group G, which yields spatial homogeneity, is just a subgroup of the full 6-dimensional symmetry group of (M, g). The additional symmetries are in general only local.

All generalized Nariai solutions can be embedded isometrically into the standard Nariai solution, at least locally. The details are given in [5]. Let us consider the universal covers in this paragraph. At the end, one may return to the original manifolds and finds that all of the following maps, which are global for the universal covers, still have at least a local meaning. One can show easily that the class of generalized Nariai solutions can be divided into three isometry classes, given by the sign of the constant

$$\sigma_0 := \Phi_0^2 - (\Phi_0')^2.$$

Consider Fig. 1. In this figure, the horizontal axis represents the ρ-coordinate and the vertical axis the coordinate τ of the universal cover of the standard Nariai solution, where

$$\tau := 2\arctan(\tanh(t/2)).$$

This compactified time coordinate has the property that $t \to \pm\infty$ corresponds to $\tau \to \pm\pi/2$. Each point in this diagram determines a 2-sphere in the standard Nariai solution. In these coordinates, null curves which are constant on the $\mathbb{S}^2$-factor are straight lines and their angles have the Minkowski value. Hence the picture appears like a Penrose

diagram. However, note that this would not be the case if we considered general null curves. In the case $\sigma_0 > 0$, the corresponding generalized Nariai solution is globally isometric to the standard Nariai solution. For $\sigma_0 = 0$, after possibly a change of time direction, the generalized Nariai solutions are isometric to region II in Fig. 1. The green curves represent its $\hat{t} = const$-surfaces and the blue curves $\hat{\rho} = const$-surfaces. Here, coordinate names with a hat are the coordinates of the generalized Nariai solution to be embedded. The black lines in the figure represent the limit $\hat{t} \to -\infty$. In the case $\sigma_0 < 0$, possibly after a change of time direction, III is the relevant region in the figure. Here, the black lines correspond to the curves $\hat{t} \to t_0$, where $t_0 \in \mathbb{R}$ is the time at which Φ becomes zero. This picture motivates the fact that for $\sigma_0 \leq 0$, all generalized Nariai solutions are causal geodesically incomplete.

After a change of time direction, if necessary, all generalized Nariai solutions have "Nariai asymptotics" to the future for large t. More details on what we mean by Nariai asymptotics are given in [5]. Certainly, there are many possible ways of characterizing Nariai asymptotics. But in geometrical language, we say that a spacetime has Nariai asymptotics to, say, the future if future late time observers are oblivious to topology, but not completely oblivious to topology in the language of Ringström [20]. The property "oblivious to topology" means that there exists a Cauchy surface which is not contained in the causal past of any late time observer. This can be interpreted as an effect of the rapid asymptotic expansion of the spacetime. It is true for the Nariai solutions. In particular, it is true for the de-Sitter spacetime, and hence, from the cosmic-no hair point of view, it is expected for generic asymptotically expanding cosmological solutions. The property "completely oblivious to topology" means that there exists a Cauchy surface Σ such that for each future directed inextendible causal curve γ the intersection of the causal past of γ and Σ is contained in a subset of Σ homeomorphic to a 3-ball in $\mathbb{R}^3$, i.e. a "topologically trivial" subset. In this situation an observer will have no information about the topology of Σ whatsoever. It is true for the de-Sitter spacetime and hence is again expected for generic cosmological solutions which are asymptotically expanding in the future, due to the cosmic-no hair conjecture. However, the Nariai solutions do not have this property. Indeed, Ringström, in [20], proves an even more detailed statement, namely, regardless of the choice of Cauchy surface Σ and future directed inextendible causal curve γ, the intersection of Σ and the causal past of γ is not contained in a set homeomorphic to a 3-ball. Loosely speaking, due to the anisotropic expansion of Nariai, the observers will always have *some* information concerning the spatial topology, although never the complete information. One consequence of this, as we proved in [5], is that the standard Nariai solution cannot have even a small piece of a smooth conformal boundary.

The above suggests that the Nariai solution is not consistent with the cosmic no-hair picture. In this paper, and in [5], the purpose was to find out if this has the consequence that the Nariai asymptotics are non-generic among solutions of Einstein's field equations by considering small perturbations of Nariai solutions. The expectation is that an arbitrary small perturbation of any Nariai data, a term which we explain below, should either not expand at all in the future or it should expand in a manner consistent

with cosmic no-hair, for instance by forming smooth future conformal boundaries. The analogous statement holds in the past time direction.

As a first step in this direction, we investigated spatially homogeneous perturbations of the family of generalized Nariai solutions in [5]. Let us give a brief summary. We consider the class of spacetimes with a manifold $M = \mathbb{R} \times (\mathbb{S}^1 \times \mathbb{S}^2)$ and a metric g which is invariant under a global smooth effective action of the Kantowski-Sachs group acting transitively on spacelike orbits. Then one can make the following general ansatz for the metric

$$g = 2dsd\mu + F(s)d\mu^2 + G(s)g_{\mathbb{S}^2}.$$

The $s = const$-hypersurfaces are the symmetry orbits and μ is the standard coordinate on the $\mathbb{S}^1$-factor. We write all solutions of Einstein's field equations in vacuum for $\Lambda = 1$ explicitly in the form

$$F(s) = F_* + \dot{F}_* s \frac{2}{H_*^{(0)} s + 2} + s^2 \frac{H_*^{(0)} s + 6}{3H_*^{(0)} s + 6},$$
$$G(s) = \frac{G_*}{4}(H_*^{(0)} s + 2)^2,$$

with constants $G_* > 0$, $F_* > 0$, $\dot{F}_*$, $H_*^{(0)}$ corresponding to the data of F and G on the initial hypersurface given for $s = 0$ by

$$F_* = F(0), \quad G_* = G(0), \quad \dot{F}_* = (\partial_s F)(0), \quad H_*^{(0)} = (\partial_s G)(0)/G(0).$$

These constants have to satisfy a constraint equation, see [5]. It turns out that any solution with $H_*^{(0)} = 0$ is an analytic extension of the generalized Nariai solution given by

$$\Phi_0 = \sqrt{F_*}, \quad \Phi_0' = \dot{F}_*/2.$$

Here, $G_* = 1$ is a consequence of the constraints. For $H_*^{(0)} \neq 0$, the solutions are locally Schwarzschild-de-Sitter solutions with mass

$$S = G_*^{3/2}\left(\frac{1}{3} - \frac{1}{4}\dot{F}_* H_*^{(0)}\right).$$

Let us fix a generalized Nariai solution (M, g) by means of the parameters $F_* > 0$, $\dot{F}_*$ and $H_*^{(0)} = 0$, called Nariai data. Any solution $(\tilde{M}, \tilde{g})$ with the same parameters F_*, $\dot{F}_*$, but with sufficiently small $|H_*^{(0)}| \neq 0$, will be referred to as a perturbation (of Nariai data). We will not give the complete instability result here. For our purposes in this paper, the case $\sigma_0 < 0$, determined by F_*, $\dot{F}_*$, is of interest. In this case, the perturbation is locally isometric to a subset of a Schwarzschild-de-Sitter solution with mass

$$0 < S < 1/3,$$

close to the critical value $1/3$ as we showed in [5]. Let us consider Fig. 2 for the corresponding Penrose diagram. Black bold lines denote the event and cosmological horizons,

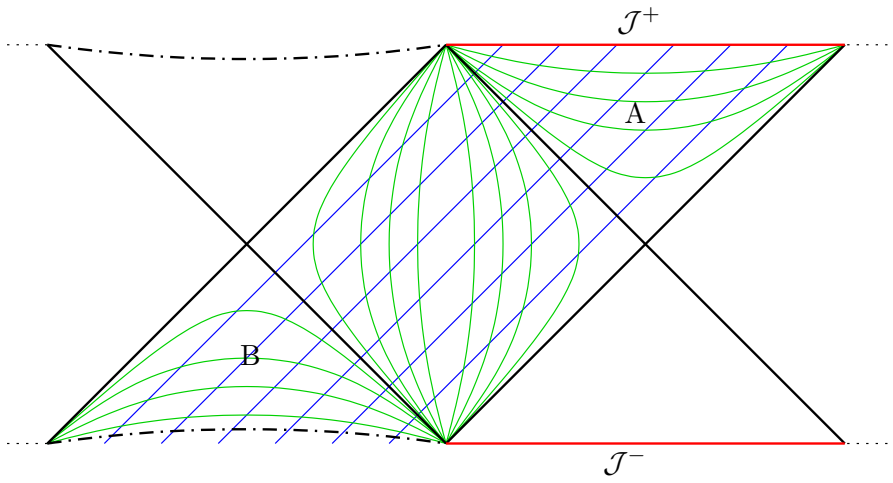

Fig. 2: Penrose diagram of Schwarzschild-de-Sitter with mass $0 < S < 1/3$ and $\Lambda = 1$

dashed black line refer to the singularity, bold red lines mark the conformal boundary $\mathcal{J}$. Furthermore, green lines represent $s = const$-hypersurfaces and blue lines $\mu = const$-hypersurfaces. We can change the time direction so that $\dot{F}_* > 0$. In [5], we demonstrated the following. If $H_*^{(0)} > 0$, then the perturbation $(\tilde{M}, \tilde{g})$ equals the region A in Fig. 2. In the future time direction, while the unperturbed Nariai solution (M, g) has Nariai asymptotics, the perturbation $(\tilde{M}, \tilde{g})$ has a smooth future conformal boundary $\mathcal{J}^+$. In other words, while for the original solution, the volume of the $\mathbb{S}^2$-factor is constant in time, an arbitrarily small initial positive expansion of the $\mathbb{S}^2$-factor determined by a small $H_*^{(0)} > 0$ leads to accelerated expansion of the $\mathbb{S}^2$-factor which is, together with the accelerated expansion of the $\mathbb{S}^2$-factor present also in the unperturbed solution, consistent with the existence of a smooth future conformal boundary $\mathcal{J}^+$. In the past, both (M, g) and the perturbation $(\tilde{M}, \tilde{g})$ develop a Cauchy horizon, which in the case of the perturbation is given by the cosmological horizon. This means that the maximal globally hyperbolic extension of the data on the $s = 0$-hypersurface is extendible. The case $H_*^{(0)} < 0$ can be discussed similarly. The relevant region in Fig. 2 is now marked as region B. For the perturbation $(\tilde{M}, \tilde{g})$, the initial expansion of the $\mathbb{S}^2$-factor is now negative, and the result is that the future Nariai asymptotics of (M, g) are substituted by a curvature singularity. Note that we have to turn the time direction around here, as can be seen from [5]. The singularity is of cigar type according to the classification in [25] because the volume of the $\mathbb{S}^1$-factor becomes infinite at the singularity. In the past, both (M, g) and $(\tilde{M}, \tilde{g})$ develop a Cauchy horizon, which in the case of the perturbation is given by the event horizon.

4 Gowdy symmetric perturbations of Nariai solutions

As mentioned before, the aim of this paper is to go beyond spatially homogeneous perturbations and to study the expected instability of the Nariai asymptotics in more general classes of solutions. Here, we restrict to the class of Gowdy symmetric solutions. General aspects about $\mathrm{U}(1) \times \mathrm{U}(1)$-symmetric solutions were first discussed in [13] and later reconsidered in [7]. We cannot present the general theory here, but list only some of the important facts.

4.1 Gowdy symmetry on spacetimes with spatial topology $\mathbb{S}^1 \times \mathbb{S}^2$

Let us consider a smooth global effective action of the group $\mathrm{U}(1) \times \mathrm{U}(1)$ on a 3-dimensional smooth compact orientable manifold. One can show, see the references in [7], that the only compatible smooth compact orientable 3-manifolds are $\mathbb{T}^3$, $\mathbb{S}^1 \times \mathbb{S}^2$, $\mathbb{S}^3$ and lens spaces. Since the universal cover of the lens spaces is $\mathbb{S}^3$, they will always be included when we speak about $\mathbb{S}^3$. In this paper, we are particularly interested in the case $\mathbb{S}^1 \times \mathbb{S}^2$. However, for the discussion of our numerical approach later, it makes sense to consider the case $\mathbb{S}^3$ simultaneously now. On $\mathbb{S}^1 \times \mathbb{S}^2$, let us consider coordinates (ρ, θ, ϕ) where $\rho \in (\mathbb{R} \bmod 2\pi)$ is the standard parameter on $\mathbb{S}^1$ and (θ, ϕ) are standard polar coordinates on $\mathbb{S}^2$

$$x_1 = \sin\theta \cos\phi, \quad x_2 = \sin\theta \sin\phi, \quad x_3 = \cos\theta. \tag{3}$$

In writing these coordinate expressions, we assume that $\mathbb{S}^2$ is embedded in the standard way into $\mathbb{R}^3$ with Cartesian coordinates (x_1, x_2, x_3). Note that in the following, we will always identify the groups $\mathbb{S}^1$, $\mathrm{U}(1)$ and $(\mathbb{R} \bmod 2\pi)$. On $\mathbb{S}^3$, we consider Euler coordinates $(\chi, \lambda_1, \lambda_2)$ with the same conventions as in [3], namely

$$\begin{aligned} x_1 &= \cos\frac{\chi}{2}\cos\lambda_1, \quad x_2 = \cos\frac{\chi}{2}\sin\lambda_1, \\ x_3 &= \sin\frac{\chi}{2}\cos\lambda_2, \quad x_4 = \sin\frac{\chi}{2}\sin\lambda_2, \end{aligned} \tag{4}$$

where we assume the standard embedding of $\mathbb{S}^3$ into $\mathbb{R}^4$ similar to the above. Here, $\chi \in [0, \pi]$ and $\lambda_1, \lambda_2 \in (\mathbb{R} \bmod 2\pi)$. In terms of these coordinates, we can write a representation of the action of the group $G = \mathrm{U}(1) \times \mathrm{U}(1)$. For $\mathbb{S}^1 \times \mathbb{S}^2$, one has

$$\Psi : G \times (\mathbb{S}^1 \times \mathbb{S}^2) \to \mathbb{S}^1 \times \mathbb{S}^2, \quad ((u_1, u_2), (\rho, \theta, \phi)) \mapsto (\rho + u_1, \theta, \phi + u_2)$$

for $(u_1, u_2) \in \mathrm{U}(1) \times \mathrm{U}(1)$ and $(\rho, \theta, \phi) \in \mathbb{S}^1 \times \mathbb{S}^2$. Hence a basis of generators of the action are the coordinate fields ∂_ρ and ∂_ϕ. These are globally smooth vector fields on $\mathbb{S}^1 \times \mathbb{S}^2$ and one can check that this action is global, smooth and effective. The action degenerates at those points where ∂_ϕ becomes zero, namely at the poles of the $\mathbb{S}^2$-factor given by $\theta = 0, \pi$. In the case of $\mathbb{S}^3$, we have the following action

$$\Psi : G \times \mathbb{S}^3 \to \mathbb{S}^3, \quad ((u_1, u_2), (\chi, \lambda_1, \lambda_2)) \mapsto (\chi, \lambda_1 + u_1, \lambda_2 + u_2).$$

The generators of the group are the coordinate fields ∂_{λ_1} and ∂_{λ_2}. Here, as well, these are globally smooth vector fields on $\mathbb{S}^3$. Indeed, the action is global, smooth and effective. The action degenerates where either ∂_{λ_1} or ∂_{λ_2} become zero, which is the case at $\chi = 0, \pi$. Now, it is a fact, quoted in [7], that all other smooth effective global actions of $\mathrm{U}(1)\times\mathrm{U}(1)$ on a given manifold must be equivalent, i.e. can only differ by an automorphism of the group or by a diffeomorphism of the manifold. Hence it is sufficient to have one representation of the action.

We will now formulate the actions above, or, more precisely, their generators, in an equivalent but more geometrical manner, i.e. not in terms of coordinates. For $\mathbb{S}^1 \times \mathbb{S}^2$, the basis of the algebra of generators of the action above equals $\{W_3, \xi_3\}$ from Eq. (2), i.e. the translation vector field along the $\mathbb{S}^1$-factor of the manifold and a rotation of the $\mathbb{S}^2$-factor of the manifold corresponding to an element of the Lie algebra of SO(3). In the $\mathbb{S}^3$-case, let us introduce the vector fields

$$\begin{aligned}
Y_1 &= 2\sin\rho_1\,\partial_\chi + 2\cos\rho_1\,(\cot\chi\,\partial_{\rho_1} - \csc\chi\,\partial_{\rho_2})\,,\\
Y_2 &= 2\cos\rho_1\,\partial_\chi - 2\sin\rho_1\,(\cot\chi\,\partial_{\rho_1} - \csc\chi\,\partial_{\rho_2})\,,\\
Y_3 &= 2\partial_{\rho_1}\,,\\
Z_1 &= -2\sin\rho_2\,\partial_\chi - 2\cos\rho_2\,(\cot\chi\,\partial_{\rho_1} - \csc\chi\,\partial_{\rho_2})\,,\\
Z_2 &= 2\cos\rho_2\,\partial_\chi - 2\sin\rho_2\,(\cot\chi\,\partial_{\rho_1} - \csc\chi\,\partial_{\rho_2})\,,\\
Z_3 &= 2\partial_{\rho_2}\,,
\end{aligned}$$

in terms of the Euler angle coordinates above, but with

$$\lambda_1 = (\rho_1 + \rho_2)/2, \quad \lambda_2 = (\rho_1 - \rho_2)/2. \tag{5}$$

These definitions are in accordance with the conventions in [4, 3], and are needed again later in this paper. These vector fields have the property that they are globally smooth on $\mathbb{S}^3$ and are invariant under the standard left- and right-actions, respectively, of the group SU(2) on $\mathbb{S}^3$. Furthermore, they satisfy

$$[Y_a, Y_b] = 2\sum_{c=1}^{3}\eta_{abc}Y_c, \quad [Z_a, Z_b] = 2\sum_{c=1}^{3}\eta_{abc}Z_c, \quad [Y_a, Z_b] = 0.$$

Here η_{abc} is the totally antisymmetric symbol with $\eta_{123} = 1$. Note that the collections $\{Y_1, Y_2, Y_3\}$ and $\{Z_1, Z_2, Z_3\}$ are global frames on $\mathbb{S}^3$. A basis of the algebra of generators of the action of the group $\mathrm{U}(1)\times\mathrm{U}(1)$ on $\mathbb{S}^3$ is clearly given by $\{Y_3, Z_3\}$. We remark that both Y_3 and Z_3 are nowhere vanishing vector fields. They become, however, collinear exactly where the action of $\mathrm{U}(1) \times \mathrm{U}(1)$ degenerates.

Recall that both $\mathbb{S}^1 \times \mathbb{S}^2$ and $\mathbb{S}^3$ are principal fiber bundles over $\mathbb{S}^2$ with structure group U(1). In the $\mathbb{S}^1 \times \mathbb{S}^2$-case, it is the trivial bundle with bundle map

$$\Phi_1 : \mathbb{S}^1 \times \mathbb{S}^2 \to \mathbb{S}^2, \quad (p, q) \mapsto q.$$

In the $\mathbb{S}^3$-case, it is the Hopf bundle and the bundle map can be given the representation

$$\begin{aligned}\Phi_2 : \mathbb{S}^3 \to \mathbb{S}^2, \quad & (x_1, x_2, x_3, x_4) \mapsto (y_1, y_2, y_3) \\ & = (-2(-x_1x_3 + x_2x_4), 2(x_2x_3 + x_1x_4), x_1^2 + x_2^2 - x_3^2 - x_4^2).\end{aligned}$$

Here the notation is such that $(x_1, x_2, x_3, x_4) \in \mathbb{S}^3 \subset \mathbb{R}^4$ with standard Cartesian coordinates on $\mathbb{R}^4$, and $(y_1, y_2, y_3) \in \mathbb{S}^2 \subset \mathbb{R}^3$. When we write this map in terms of the Euler angle coordinates for $\mathbb{S}^3$, given by Eqs. (4) and (5), and polar coordinates on $\mathbb{S}^2$ given by Eq. (3) (with x_i substituted by y_i), then the Hopf map has the simple representation

$$\Phi_2 : (\chi, \rho_1, \rho_2) \mapsto (\theta, \phi) = (\chi, \rho_1).$$

In order to simplify notation we write

1. $M := \mathbb{S}^1 \times \mathbb{S}^2$ or $\mathbb{S}^3$,
2. $\eta := \xi_3$ or Z_3, $\quad \sigma := 2W_3$ or Y_3,
3. $\Phi := \Phi_1$ or Φ_2,

in the following. Furthermore, we write $G = \mathrm{U}(1) \times \mathrm{U}(1)$ and $G_1 = \mathrm{U}(1)$ the subgroup of G which is generated by η. Recall that η is nowhere vanishing and note that its integral curves are closed circles. We notice that in both cases, the field η is tangent to the fibers of the bundles, and hence G_1 becomes the structure group. In particular, $M/G_1 \cong \mathbb{S}^2$. Note that, in particular, $\Phi_*\sigma$ is a smooth global vector field on $\mathbb{S}^2$, and indeed equals the coordinate vector field $2\partial_\phi$ in both cases, which demonstrates even further how similar both cases are from this point of view.

Now let us consider the following situation. Assume that we want to solve a set of partial differential equations on M, possibly with an additional time function t, such that all unknowns and coefficients are smooth functions on M which are constant along η and such that all differential operators in the equations originate in smooth vector fields on M whose Lie brackets with η vanish. Then there is an equivalent system of equations on $\mathbb{S}^2$ as follows. Each such unknown and coefficient can be identified uniquely with a smooth function on $\mathbb{S}^2$. Furthermore, each such vector field yields a unique smooth vector field on $\mathbb{S}^2$ (which certainly has zeros). Most importantly, the solution of these new equations on $\mathbb{S}^2$, if it exists, hence yields a unique corresponding solution of the original problem on M. Thus there is no loss of information when we "transport the problem from M to $\mathbb{S}^2$".

From now on, let us restrict to the case $M = \mathbb{S}^1 \times \mathbb{S}^2$ and consider smooth Riemannian metrics on M which are invariant under G. First, one can show that without loss of generality, the metric can be parametrized as

$$h = e^{2\lambda} d\theta^2 + R(e^P d\phi^2 + 2e^P Q d\phi\, d\rho + (e^P Q^2 + e^{-P}) d\rho^2), \tag{6}$$

i.e. ∂_θ can be assumed to be orthogonal to the group orbits everywhere. Here, all functions involved only depend on θ. For the smoothness of h, it turns out to be sufficient

and necessary that there are function $\tilde{R}, \tilde{P}, \tilde{\lambda}$ such that

$$R = \tilde{R} \sin\theta, \tag{7a}$$

$$P = \tilde{P} + \ln \sin\theta, \tag{7b}$$

$$\lambda = (\tilde{P} + \ln \tilde{R})/2 + \tilde{\lambda}, \tag{7c}$$

where $\tilde{R}$, $\tilde{P}$, $\tilde{\lambda}$ and Q are smooth function of $\cos\theta$ and

$$\tilde{\lambda}\Big|_{\theta=0,\pi} = 0. \tag{7d}$$

This fact was shown in [7] and applied for instance in [12]. But one can redo the proof in a more global fashion by first writing a general smooth metric in terms of a smooth global frame, e.g.

$$V_1 = 2(-x_1\partial_\rho + W_1), \quad V_2 = 2(x_2\partial_\rho + W_2), \quad V_3 = 2(x_3\partial_\rho + W_3), \tag{8}$$

second by solving the Killing equations in terms of the frame coefficients of the metric, and finally by turning to the coordinate expression of the metric by means of the coordinate expressions of the frame. In the case of $\mathbb{S}^3$, one finds similar, but distinct results.

Now let us consider a globally hyperbolic spacetime (M, g) foliated with Gowdy invariant Cauchy surfaces of topology $\mathbb{S}^1 \times \mathbb{S}^2$, i.e. the first and second fundamental form of each surface are invariant under the action of G. It has been shown before [7, 8] that if this spacetime is a solution of Eq. (1), the action of the Gowdy group is orthogonally transitive, i.e. the twist constants

$$c^1 := \epsilon^{\mu\nu\sigma\lambda}\eta^1_\mu\sigma^2_\nu\partial_\sigma\eta^a_\lambda, \quad c^2 := \epsilon^{\mu\nu\sigma\lambda}\eta^1_\mu\sigma^2_\nu\partial_\sigma\sigma^a_\lambda$$

vanish. Here all index manipulations are done with the metric g and ϵ is the volume form of g assuming a suitable choice of orientation. See also [25] for more details. Then, solutions of spatial topology $\mathbb{S}^1 \times \mathbb{S}^2$ or $\mathbb{S}^3$, which are $\mathrm{U}(1) \times \mathrm{U}(1)$-symmetric, are called Gowdy solutions [13].

It is clear that from the point of view of an initial value problem, not all coordinate gauge conditions, i.e. not all choices of lapse and shift, are consistent with the assumption that for all $t = const$-hypersurfaces, the first and second fundamental form are symmetry invariant and that the Killing vector fields can be identified with the coordinate vector fields ∂_ρ and ∂_ϕ for all times. Most prominent examples of – in this sense – consistent gauges are the so-called areal gauge and the "conformal gauge"[1]; for more information see for instance [8]. A further candidate of interest is Gauss gauge, and this is the gauge condition of our choice in this work. In this gauge, the metric g takes the form

$$g = -dt^2 + h \tag{9}$$

[1]Conformal gauge must not be confused with the conformal approach described in Section 6.1.

with h given by Eq. (6) together with Eqs. (7). We do not write Einstein's field equations for the coordinate functions $\tilde{R}$, $\tilde{P}$, Q and $\tilde{\lambda}$ in these gauges here, since this has been done elsewhere often enough, see the reference above, and since these formulations of the equations are not used in the present paper. Our formulation is given in Section 6.1.

Finally, let us make a remark concerning the spatially homogeneous case. If (M, g) is spatially homogeneous then the metric is in Gauss gauge

$$g = -dt \otimes dt + \tilde{R}e^{\tilde{P}}(d\theta \otimes d\theta + \sin^2\theta d\phi \otimes d\phi) + \tilde{R}e^{-\tilde{P}}d\rho \otimes d\rho.$$

In the following we will also use the representation of the metric in "conformal gauge"

$$g = \tilde{R}e^{\tilde{P}}(-dt \otimes dt + d\theta \otimes d\theta) + \tilde{R}e^{\tilde{P}}\sin^2\theta d\phi \otimes d\phi + \tilde{R}e^{-\tilde{P}}d\rho \otimes d\rho. \tag{10}$$

All function in this metric only depend on t. Note that in this conformal gauge, the generalized Nariai metrics are determined by

$$\tilde{R}(t) = \Phi(t)/\Lambda, \quad \tilde{P}(t) = -\ln\Phi(t). \tag{11}$$

4.2 Setup for Gowdy symmetric perturbations of Nariai

We would like to study Gowdy symmetric solutions close to generalized Nariai spacetimes. This means that, given a Nariai initial data set, we want to study the future and past time asymptotics of the solutions corresponding to small perturbations of these initial data.

Before we construct Gowdy symmetric initial data close to Nariai initial data in Section 5, let us tackle the following question. Recall that, in the spatially homogeneous case, the initial value of the expansion $H_*^{(0)}$ of the $\mathbb{S}^2$-factor of the manifold played the central role from the point of view of studying the instability of Nariai asymptotics. However, there is no such canonical quantity in the spatially inhomogeneous case. First, there is no canonical foliation of spacetime, and, second, no geometrically preferred "$\mathbb{S}^2$-factor".

However, we choose Gauss gauge, and for small perturbations of Nariai data, the expansion of the "coordinate $\mathbb{S}^2$-factor" can be hoped to play a role similar to that of $H_*^{(0)}$ in the spatially homogeneous case. By the "coordinate $\mathbb{S}^2$-factor", we will always mean the following. On the initial hypersurface, we choose coordinates (ρ, θ, ϕ) as before. By means of the gauge conditions, these spatial coordinates are transported to all $t = const$-hypersurfaces. On any $t = const$-hypersurface, the "coordinate $\mathbb{S}^2$-factor" is then a 2-surface diffeomorphic to $\mathbb{S}^2$ determined by $\rho = const$. Since the metric is invariant under translation along ρ, all such 2-surfaces are isometric at a given t. Similarly we define the coordinate $\mathbb{S}^1$-factor. However, here its geometric properties depend on the point on the given $t = const$-hypersurface.

The relevant expansions are defined as follows for Gauss gauge. Let H be the mean curvature of any $t = const$-hypersurface. Let H_2 be the projection of the mean curvature

vector of a coordinate $\mathbb{S}^2$-factor to ∂_t. Similarly, we define H_1 as the expansion of the coordinate $\mathbb{S}^1$-factor. The following formulas hold.

$$H = \frac{3\tilde{R}' + \tilde{R}\left(\tilde{P}' + 2\tilde{\lambda}'\right)}{6\tilde{R}} \tag{12a}$$

$$H_2 = \frac{\tilde{R}' + \tilde{R}\left(\tilde{P}' + \tilde{\lambda}'\right)}{2\tilde{R}} \tag{12b}$$

$$3H - 2H_2 - H_1 = -\frac{e^{2\tilde{P}} Q \sin^2\theta \left(Q\tilde{P}' + Q'\right)}{1 + e^{2\tilde{P}} Q^2 \sin^2\theta}, \tag{12c}$$

where a prime denotes a derivative with respect to Gaussian time. In this paper, we will study in particular, if the quantity H_2 has properties similar to $H_*^{(0)}$ in the spatially homogeneous case.

5 Our choice of initial data

Our aim is now to find families of Gowdy invariant initial data. These are solutions of the constraint equations implied by the vacuum Einstein's field equations with $\Lambda > 0$ on a Cauchy surface of $\mathbb{S}^1 \times \mathbb{S}^2$-topology. These data should comprise Nariai initial data and data which are close in some sense, which could hence be interpreted as perturbations of Nariai data.

Let t be the time coordinate of the "conformal gauge" mentioned earlier. We use this time coordinate of the conformal gauge to express the constraint equations. There is no particular reason to do so and it might actually be confusing for the reader. However, the data which we write with respect to this time coordinate can easily be transformed to the Gauß time coordinate, which we will use for the evolutions. The constraints are

- Hamiltonian constraint:

$$0 = \frac{1}{4}P'^2 + \frac{1}{4}e^{2P}Q'^2 - \frac{R'^2}{4R^2} + \frac{1}{4}\dot{P}^2 + \frac{1}{4}e^{2P}\dot{Q}^2 - \frac{\dot{R}^2}{4R^2} + e^{2\lambda}\Lambda - \frac{R'\lambda'}{R} + \frac{R''}{R} - \frac{\dot{R}\dot{\lambda}}{R},$$

- Momentum constraint

$$0 = \frac{1}{2}P'\dot{P} + \frac{1}{2}e^{2P}Q'\dot{Q} - \frac{R'\dot{R}}{2R^2} - \frac{\lambda'\dot{R}}{R} - \frac{R'\dot{\lambda}}{R} + \frac{\dot{R}'}{R}.$$

A dot represents a t-derivative and a prime a θ-derivative. We assume that on the initial hypersurface, the action of the Gowdy group is of the standard form, which implies that the quantities R, P, Q, λ must be expressible via Eqs. (7). When the new quantities $\tilde{R}$, $\tilde{P}$ and $\tilde{\lambda}$ are substituted into the constraint equations, formally singular expressions arise. In this paper, we do not address the question of how to deal with these formally singular expressions in a general solution procedure of the constraints; another publication which

is currently in progress is devoted to such and related issues. In the case $\Lambda = 0$, the corresponding problem has been addressed in [12]. For $\Lambda > 0$, however, the additional term $e^{2\tilde{\lambda}}\Lambda$ has the effect that Eq. (14) in [12] must be substituted by a more complicated condition. Otherwise, the same complications due to the nature of the singular terms in the constraints arise as in the case $\Lambda = 0$. In the present paper, we will be satisfied with a particular family of explicit solutions of the constraints with the properties mentioned above. In all of what follows, we will assume $\Lambda = 3$ without loss of generality.

We have mentioned before that the functions $\tilde{R}$, $\tilde{P}$, Q and $\tilde{\lambda}$ must be smooth functions of $\cos\theta$ and $\tilde{\lambda}$ has to become zero at $\theta = 0, \pi$. Now we make a polynomial ansatz for these functions in $z = \cos\theta$, solve the constraints for the polynomial coefficients and try to match these boundary conditions. In this way, which requires cumbersome algebra which we did with Mathematica, we have come up with the following family of Gowdy symmetric solutions of the constraints

$$\tilde{R} = \tilde{R}_*, \quad \tilde{R}' = \frac{\tilde{R}_*}{\kappa}, \tag{13a}$$

$$\tilde{P} = P_* - \frac{\sqrt{3}}{2\kappa}\tilde{N}_\times^{(1)}\sin^2\theta, \quad \tilde{P}' = \frac{\sqrt{3}}{\kappa}(\Sigma_-^{(0)} - \Sigma_\times^{(1)}\cos^2\theta), \tag{13b}$$

$$Q = -\frac{\sqrt{3}}{\kappa}\tilde{N}_\times^{(1)}\int_{-1}^{\cos\theta} e^{-\tilde{P}(z)}dz, \quad Q' = \frac{\sqrt{3}}{\kappa}\Sigma_\times^{(1)}e^{-\tilde{P}}, \tag{13c}$$

$$\tilde{\lambda} = \frac{\sqrt{3}}{4\kappa}\tilde{N}_\times^{(1)}\sin^2\theta, \quad \tilde{\lambda}' = \frac{\sqrt{3}}{2\kappa}(\sqrt{3}\Sigma_+^{(2)} - \Sigma_\times^{(1)})\sin^2\theta. \tag{13d}$$

The constants P_*, $\tilde{N}_\times^{(1)}$, $\Sigma_+^{(2)}$ are determined transcendentally by the actual initial data parameters $(\tilde{R}_*, \kappa, \Sigma_-^{(0)}, \Sigma_\times^{(1)})$ in the following manner. Let us make the abbreviation

$$C := \frac{1}{\sqrt{3}\,\kappa}\sqrt{\kappa^4 + \left(3(\Sigma_\times^{(1)})^2 - 6\Sigma_-^{(0)}\Sigma_\times^{(1)} + 2\sqrt{3}\Sigma_-^{(0)}\right)\kappa^2 + 3(\Sigma_\times^{(1)} - \Sigma_-^{(0)})^2}.$$

Then

$$P_* = \ln\left[\frac{1}{4\tilde{R}_*\kappa^2}\left(\frac{2\kappa^2}{3} - \frac{2C\kappa}{\sqrt{3}} - (\Sigma_\times^{(1)})^2 - (\Sigma_-^{(0)})^2 + 2\Sigma_\times^{(1)}\Sigma_-^{(0)} + 1\right)\right],$$

$$\tilde{N}_\times^{(1)} = \frac{\Sigma_\times^{(1)} - \Sigma_-^{(0)}}{\kappa} - C - \frac{\kappa}{\sqrt{3}},$$

$$\Sigma_+^{(2)} = \frac{3(\Sigma_\times^{(1)})^2 - 6\Sigma_-^{(0)}\Sigma_\times^{(1)} + 3C\kappa(\Sigma_-^{(0)} - \Sigma_\times^{(1)}) + \Sigma_-^{(0)}\left(\sqrt{3}\kappa^2 + 3\Sigma_-^{(0)}\right)}{3\kappa^2}.$$

From this we easily see that there are restrictions for the choice of the (otherwise free) parameters $(\tilde{R}_*, \kappa, \Sigma_-^{(0)}, \Sigma_\times^{(1)})$. We do not discuss them now. In the actual applications, we always check explicitly that these conditions are satisfied without further notice.

Let us suppose that all quantities in Eqs. (13) are well defined. The only non-explicit expression is the integral for Q, which cannot be solved explicitly when $\Sigma_\times^{(1)} \neq 0$. We

compute this integral numerically by evaluating the integral of the truncated Taylor series of the exponential function. In practice it has turned out that 20 terms in the Taylor series yields sufficient precision.

For which values of the parameters are the corresponding data spatially homogeneous? Which parameters correspond to Nariai data? Recall the spatially homogeneous case in Eq. (10). We see that we must have $\Sigma_\times^{(1)} = \tilde{N}_\times^{(1)} = \Sigma_+^{(2)} = 0$. In particular, the free parameter $\Sigma_\times^{(1)}$ will play the role of the inhomogeneity parameter of our data. In total, this yields that precisely for

$$\Sigma_-^{(0)} \leq -\frac{\kappa^2}{\sqrt{3}}, \quad \Sigma_\times^{(1)} = 0, \tag{14}$$

data given by Eqs. (13) are spatially homogeneous. This implies that our explicit family of data does not comprise all spatially homogeneous data. In particular, for any generalized Nariai data, we must have due to Eq. (11),

$$\tilde{R}_* = \Phi_*/\Lambda, \quad \kappa = \Phi_*/\Phi'_*, \quad \Sigma_-^{(0)} = -1/\sqrt{3}, \quad \Sigma_\times^{(1)} = 0.$$

However, in this case, the condition Eq. (14) implies that

$$\kappa^2 \leq 1,$$

and thus only all generalized Nariai $\sigma_0 \leq 0$ are allowed. This can be seen as a bad feature of our data, and indeed our results based on these data will be limited. It is clear anyway that this 4-dimensional family of initial data cannot be considered as generic; in particular, they do not yield generic perturbations of Nariai data. In future work, we will discuss the question of constructing general Gowdy initial data on $\mathbb{S}^1 \times \mathbb{S}^2$. However, for the time being, we see these investigations as first steps and hence use this simple family of data.

Finally, let us remark that these data are not polarized Gowdy data. This is motivated by the fact that Q is in general non-vanishing. However, this statement must be proven separately.

6 Formulation of the initial value problem

In the following, we want to describe very briefly our formulation of the evolution equations, the choice of unknowns and of the gauge. After that, our numerical approach to solve these equations is discussed. Finally we describe how to transform the initial data in Section 5 for the unknowns $\tilde{R}$, $\tilde{P}$, Q and $\tilde{\lambda}$ to our new unknowns to be introduced now.

6.1 Formulation of Einstein's field equations

A possible approach in writing evolution equations from Einstein's field equations taken in [12], is to formulate them in terms of the coordinate components of the metric expressed in terms of $\tilde{R}$, $\tilde{P}$, Q and $\tilde{\lambda}$. Numerical problems arise due to the presence of

formally singular terms at $\theta = 0, \pi$. Our alternative approach, by which we mean both the formulation of the field equations and the numerical techniques, was discussed in [4, 3]. Clearly, we cannot get rid of these singularities, but using smooth global orthonormal frames together with our spectral numerical technique allows us to control them in a simple geometric manner. A further motivation for using this approach was that the conformal techniques underlying our formulation of the evolution equations allow us, in principle, to compute the complete solution, including conformal boundaries. Recall the role of smooth conformal boundaries in our discussion of Nariai asymptotics and the cosmic no-hair picture above.

The physical metric, i.e. the solution of the field equations, is denoted in the following by $\tilde{g}$, and all corresponding quantities (connection coefficients, curvature tensor etc.) are marked with a tilde. Since we use Friedrich's conformal field equations (CFE) (as reviewed for instance in [10]), we work with the so-called conformal metric g; all corresponding quantities are written without a tilde. Both metrics are related by $g = \Omega^2 \tilde{g}$, where $\Omega > 0$ is a conformal factor. We cannot give neither further explanations here concerning these equations, nor on conformal extensions in general, see the reference above.

We will use Friedrich's general conformal field equations in a special conformal Gauss gauge [10, 9]. Up to parametrization of the timelines, our special choice of conformal Gauss gauge with time coordinate t is equivalent to (physical) Gauss gauge with time coordinate $\tilde{t}$, related by

$$t = \frac{2e^{\tilde{t}}}{1 + e^{\tilde{t}}} \quad \Leftrightarrow \quad \tilde{t} = \ln \frac{t}{2 - t}.$$

If a smooth past conformal boundary $\mathcal{J}^-$ exists, is compact with topology $\mathbb{S}^1 \times \mathbb{S}^2$ in our case, and if the solution extends to the conformal boundary in this gauge, then $\mathcal{J}^-$ is given by the $t = 0$-hypersurface. Analogously, $\mathcal{J}^+$ is represented by the $t = 2$-hypersurface. We now write the evolution equations and list the unknowns. We always assume $\Lambda = 3$ in order to obtain the simplest expressions as possible. Part of the unknown fields is a smooth frame $\{e_i\}$, which is orthonormal with respect to g, and which we represent as follows. Due to our gauge choice, we can fix

$$e_0 = \partial_t$$

which is henceforth the future directed unit normal, with respect to g, of the $t = const$-hypersurfaces. Furthermore, we write

$$e_a = e_a{}^b V_b, \tag{15}$$

where $(e_a{}^b)$ is a smooth 3×3-matrix valued function with non-vanishing determinant on $\mathbb{S}^1 \times \mathbb{S}^2$. The vector fields V_a defined in Eq. (8), where we assume standard coordinates (ρ, θ, ϕ) on every $t = const$-hypersurface, form a smooth global frame on $\mathbb{S}^1 \times \mathbb{S}^2$. Having fixed the residual gauge initial data, as described in [2], a hyperbolic reduction of the

general conformal field equations is, in this gauge, given by

$$\partial_t e_a{}^c = -\chi_a{}^b e_b{}^c, \tag{16a}$$
$$\partial_t \chi_{ab} = -\chi_a{}^c \chi_{cb} - \Omega E_{ab} + L_{ab}, \tag{16b}$$
$$\partial_t \Gamma_a{}^b{}_c = -\chi_a{}^d \Gamma_d{}^b{}_c + \Omega B_{ad} \epsilon^b{}_c{}^d, \tag{16c}$$
$$\partial_t L_{ab} = -\partial_t \Omega\, E_{ab} - \chi_a{}^c L_{cb}, \tag{16d}$$
$$\partial_t E_{fe} - D_{e_c} B_{a(f} \epsilon^{ac}{}_{e)} = -2\chi_c{}^c E_{fe} + 3\chi_{(e}{}^c E_{f)c} - \chi_c{}^b E_b{}^c g_{ef}, \tag{16e}$$
$$\partial_t B_{fe} + D_{e_c} E_{a(f} \epsilon^{ac}{}_{e)} = -2\chi_c{}^c B_{fe} + 3\chi_{(e}{}^c B_{f)c} - \chi_c{}^b B_b{}^c g_{ef}, \tag{16f}$$
$$\Omega(t) = \frac{1}{2}\, t\,(2-t), \tag{16g}$$

for the unknowns

$$u = \left(e_a{}^b, \chi_{ab}, \Gamma_a{}^b{}_c, L_{ab}, E_{fe}, B_{fe} \right). \tag{16h}$$

The unknowns are the spatial components $e_a{}^b$ of a smooth frame field $\{e_i\}$ as in Eq. (15), with $e_0 = \partial_t$, which is orthonormal with respect to the conformal metric g, the spatial frame components of the second fundamental form χ_{ab} of the $t = const$-hypersurfaces with respect to e_0, the spatial connection coefficients $\Gamma_a{}^b{}_c$, given by $\Gamma_a{}^b{}_c e_b = \nabla_{e_a} e_c - \chi_{ac} e_0$ where ∇ is the Levi-Civita covariant derivative operator of the conformal metric g, the spatial frame components of the Schouton tensor L_{ab}, which is related to the Ricci tensor of the conformal metric by

$$L_{\mu\nu} = R_{\mu\nu}/2 - g_{\mu\nu} g^{\rho\sigma} R_{\rho\sigma}/12,$$

and the spatial frame components of the electric and magnetic parts of the rescaled conformal Weyl tensor E_{ab} and B_{ab} [10, 11], defined with respect to e_0. In this special conformal Gauss gauge, the timelike frame field e_0 is hypersurface orthogonal, i.e. χ_{ab} is symmetric. In order to avoid confusions, we point out that, in general, the conformal factor Ω is part of the unknowns in Friedrich's formulation of the CFE. However, for vacuum with arbitrary Λ and for arbitrary conformal Gauss gauges, it is possible to integrate its evolution equation explicitly [9], so that Ω takes the explicit form Eq. (16g) for our choice of gauge. We note further that, E_{ab} and B_{ab} are tracefree by definition. Hence we can get rid of one of the components of each tensor, for instance by substituting $E_{33} = -E_{11} - E_{22}$; we do the same the same for the magnetic part. Certainly, this choice not motivated geometrically. The evolution equations Eqs. (16e) and (16f) of E_{ab} and B_{ab} are derived from the Bianchi system [10]. In our gauge, the constraint equations implied by the Bianchi system take the form

$$D_{e_c} E^c{}_e - \epsilon^{ab}{}_e B_{da} \chi_b{}^d = 0, \quad D_{e_c} B^c{}_e + \epsilon^{ab}{}_e E_{da} \chi_b{}^d = 0. \tag{17}$$

Here, ϵ_{abc} is the totally antisymmetric symbol with $\epsilon_{123} = 1$, and indices are shifted by means of the conformal metric. The other constraints of the full system above are equally important, but are ignored for the presentation here. Further discussions of the above evolution system and the quantities involved can be found in the references above.

Note that in Eqs. (16e), (16f) and (17), the fields $\{e_a\}$ are henceforth considered to be spatial differential operators, using Eq. (15) and writing the fields $\{V_a\}$ as differential operators in terms of coordinates according to Eq. (8) and (2). Seen as partial differential equations, these evolution equations are symmetric hyperbolic and the initial value problem is well-posed.

Friedrich's CFE allow us to use $\mathcal{J}^+$, i.e. the future conformal boundary given by $t = 2$ (or in the same way $\mathcal{J}^-$), as the initial hypersurface, restricting to classes of solutions where this surface exists. This particular initial value problem was considered in [3]. However, in our present application, the solutions subject to investigations might not even have smooth conformal boundaries. Instead, we will always choose $t = 1$, i.e. a Cauchy surface of the solution as the initial hypersurface. Nevertheless, the hope is that this setup allows to compute the complete solution including $\mathcal{J}$, if it exists.

In [4] we discussed that there is no smooth frame on $\mathbb{S}^1 \times \mathbb{S}^2$ which is globally defined such that each frame vector field has vanishing Lie brackets with both Gowdy Killing vector fields ∂_ρ and ∂_ϕ. It is only possible for one of the Killing vector fields and we choose ∂_ρ. This has the consequence that the frame components of all tensor fields derived from a Gowdy invariant metric g have non-trivial dependence on the coordinate ϕ. However, it turns out that it is possible to evaluate the ϕ-derivative of every relevant unknown at, say, $\phi = 0$ algebraically in terms of the unknowns, and hence write an evolution system with only θ-derivatives in space valid at $\phi = 0$. The resulting system, which we call $1 + 1$-system in [4] for spatial $\mathbb{S}^3$-topology, but which has the same form for $\mathbb{S}^1 \times \mathbb{S}^2$-topology according to our discussion in Section 4.1, is symmetric hyperbolic. We refer to this system as the $1 + 1$-reduction and use this system exclusively in all of what follows in this paper.

6.2 Numerics

We discussed in Section 4.1 that for Gowdy symmetry, spatial $\mathbb{S}^1 \times \mathbb{S}^2$- and $\mathbb{S}^3$-topology have exactly the same representation from our geometrical point of view. Basically, we only need to substitute the coordinates (χ, ρ_1, ρ_2) in the $\mathbb{S}^3$-case by the coordinates (θ, ϕ, ρ) in the $\mathbb{S}^1 \times \mathbb{S}^2$-case. Nevertheless, these two situations have different properties in so far as both cases require different initial data components and orthonormal frames for topological reason. However, apart from that, it is possible to use the same numerical technique as that described in [4].

Let us repeat the main ingredients of the code for the case of spatial $\mathbb{S}^3$-topology and the underlying geometrical idea of [4] quickly. By means of the Euler coordinates of $\mathbb{S}^3$, it is possible transport partial differential equations on $\mathbb{S}^3$ to $\mathbb{T}^3$; loosely speaking, we make "all spatial directions periodic". It is clear that such a map must be singular at some places. In any case, on the one hand, this geometric approach allows to apply Fourier based pseudospectral spatial discretization. Furthermore, because of the singular structure of that map, the Fourier series of functions originating in smooth function on $\mathbb{S}^3$, must have special properties, listed in [4]. It turns out that this knowledge allows to compute the coefficients of the Fourier series of all formally singular terms in the equations explicitly from the Fourier coefficients of the unknowns. This makes it possible

to extrapolate explicitly all formally singular terms to the locations of the coordinate singularities in a reliable, and, in our experience numerically stable manner. Nevertheless, in practice it turned out to be necessary to introduce our method of "boundary enforcing" [4], in order to guarantee this numerical stability. In all our present applications, however, these kinds of errors were so small and converging to zero with increasing resolution, that this technique was not used.

We used the spatial adaption technique described in [4]. After some experiments, the quantity χ_{22} was chosen as the reference variable.

For the time evolution, we use the method of lines. In this work, all numerical results were obtained with the adaptive 5th-order "embedded" Runge Kutta scheme from [19]. Later, we will mention the parameter η, also introduced in [4], which controls the required accuracy of the time integration; the lower its value is, the smaller the time steps are chosen by the adaption algorithm.

6.3 Computing initial data

For our formulation of the field equations, the initial data consist of the quantities u, defined in Eq. (16h), on the initial hypersurface given by $t = 1$. All these quantities are expressed with respect to the orthonormal frame $\{e_i\}$. In Section 5, we constructed initial data for the functions $\tilde{R}$, $\tilde{P}$, Q and $\tilde{\lambda}$. But neither we fixed data for the initial value of the frame, i.e. the components ${e_a}^b$ in Eq. (15), nor we computed the corresponding initial values of u. Note that in order to compute u at $t = 1$ from these data, we need the first and second time derivatives of the data. Nevertheless, we only require the value of ${e_a}^b$ at $t = 1$, hence no time derivatives of the frame components, for computing u.

The main remaining tasks are now to, first, choose an orthonormal frame, i.e. its spatial part, at $t = 1$, and, second, to compute the values u at $t = 1$ from the family of Gowdy invariant initial data described in Section 5. We choose the initial value of the spatial frame as follows. For the parametrized family of initial data constructed in Section 5, consider the frame $\{V_a\}$ in Eq. (8) and perform a Gram-Schmidt orthonormalization with respect to the initial conformal 3-metric. More precisely, we construct the matrix $({e_a}^b)$ from Eq. (15) as an upper triangular matrix. For instance, this means that e_3 and V_3 are collinear initially. Of course there is a huge freedom of choosing frames, and our particular choice actually turns out to be simple minded. The reason is that with such a frame, the initial data quantities, although they are smooth functions, they require a very high spatial resolution, in order for the numerical errors, in computing u, to decrease to an acceptable level. It is clear anyway that with such an orthonormal frame, even spatially homogeneous initial data will have non-trivial spatial dependence. Besides the obvious practical difficulties implied by that, we want to stress the nice fact that at least this allows us to use spatially homogeneous solutions as non-trivial testbeds for our code.

In any case, let us proceed by making the following comments concerning computing the initial values of u from the given data. From the data in Section 5 we can compute all spatial derivatives of the initial metric components and the first time derivatives. In order to compute the initial data of the electric and magnetic parts of the rescaled

Weyl tensor for instance, we require additionally second time derivatives. We compute these by imposing the evolution equations of Einstein's field equations at $t = 1$. In all these computations the metric functions of the initial data yield formally singular terms at $\theta = 0, \pi$. We could compute these terms explicitly from the given formulas. However, in the future we would like to use the same numerical setup also for data which have been found, say, numerically and explicit expressions are thus not available. Hence we decided to make all these computations numerically. We successfully compute these formally singular terms by applying the spectral approach described above in the context of the evolution equations. Also, we compute spatial derivatives numerically with our spectral infrastructure. In practice, we find that this allows us to resolve the data u with spectral accuracy. However, due to the bad properties of the choice of frame mentioned above, large spatial resolutions are required. It is not a problem in practice to reach these large resolutions, but it turns out that round-off errors, i.e. errors introduced by the finite number representation in the computer, often yield the largest error contribution. This is true in particular when the standard "double precision" with round-off errors of the order 10^{-16} on Intel processors is used. This was our motivation to compute the initial data with "quad precision" of the Intel Fortran compiler [15], where numbers are represented with roughly 32 digits, but which is software emulated and hence relatively slow. For the evolution we still choose double precision. All our numerical computations presented here have been done this way and it has turned out to be very successful.

Finally, let us mention that for these data and this choice of orthonormal frame coefficients, the orthonormal frame is boundary adapted in the sense of [4], an issue, which is, however, of no further importance for our investigations here.

7 Numerical results

Before we actually did the numerical runs we performed various tests with the code in addition to those already reported on in [4]. Recall that with our choice of orthonormal frame, even spatially homogeneous solutions appear inhomogeneous in the sense that many of the unknowns in our equations depend on the spatial coordinates. Spatially homogeneous solutions hence yield a non-trivial test case for the code. The result is that the code is able to reproduce these solutions with promisingly small errors, in particular the Nariai solution itself. Furthermore, these errors are converging to zero up to errors which we interpret as originating in round-off errors.

Now let us discuss our choices of initial data. As the reference Nariai solution we choose the one given by $\tilde{R}_* = 1.0$, $\kappa = 0.5$ corresponding to a generalized Nariai solution with $\sigma_0 < 0$. These two parameters will be kept fixed in all of what follows. In order to perturb the data in an inhomogeneous manner, we choose first the inhomogeneity parameter $\Sigma_\times^{(1)} = 4 \cdot 10^{-4}$. We have indeed played with this parameter; in a large range of values there is no qualitative change in the following results. However, when we go to very large values of the parameter, then a different phenomenology seems to show up; this will be discussed in another paper which is currently in progress. Note that if we wanted to go to even smaller values of this parameter, we would have problems with

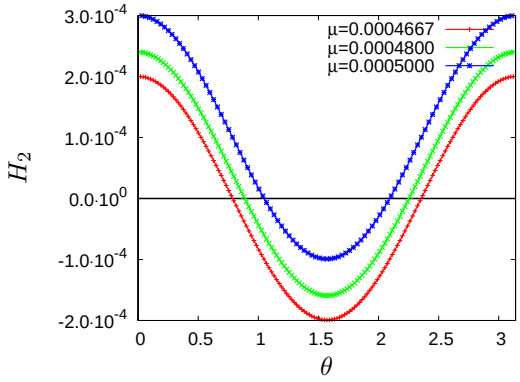

Fig. 3: Initial spatial dependence of H_2 for the three initial data sets considered here

numerical accuracy; a particular limitation would be the round-off errors, and a similar situation was discussed in [3]. In this paper, we fix $\Sigma_\times^{(1)}$ to the above value. Secondly, we introduce a small parameter μ by

$$\Sigma_-^{(0)} = -1/\sqrt{3} + \mu,$$

and choose μ so that the initial value of the quantity H_2 in Eqs. (12) has positive and negative parts, see Fig. 3. Indeed, in all of what follows, we show results for three different values of μ, namely

$$\mu = 0.0004667, \quad 0.0004800, \quad 0.0005000,$$

which are marked in all following plots by the colors red, green and blue, respectively. Recall that $\mu = \Sigma_\times^{(1)} = 0$ yields the unperturbed Nariai solution. These data are considered as small inhomogeneous perturbations of Nariai data. Changing the value of μ in this way, but leaving $\Sigma_\times^{(1)}$ fixed, has the effect that the initial spatial profiles of H_2 are "shifted vertically" in Fig. 3 without changing the shape and the amplitude of the curve; at least approximately. Our naive expectation, based on our understanding of the spatially homogeneous case, would be that the solution collapses and forms a singularity in the future at those spatial places where $H_2 < 0$ and would expand and form a smooth piece of $\mathcal{J}^+$ at those spatial places where $H_2 > 0$.

Our numerical setup has been described in Section 6.2. Here we list a few more details for the future evolution of the data given by $\mu = 0.00048$ as an example. The run is started with a spatial resolution of 300 grid points and the spatial adaption technique described before was used with a threshold value of 10^{-10}. It turned out that until the time $t = 1.99$, where this run was stopped, no spatial adaption was necessary. For the time integration, we use the adaptive Runge Kutta technique described before with an initial time step of 10^{-6} and a quality parameter $\eta = 10^{-15}$. At early times, the time step increased to roughly 10^{-3}, but at late times, very close to the final time, it reached the value 10^{-8}. With one exception below, we will only present our numerical results for

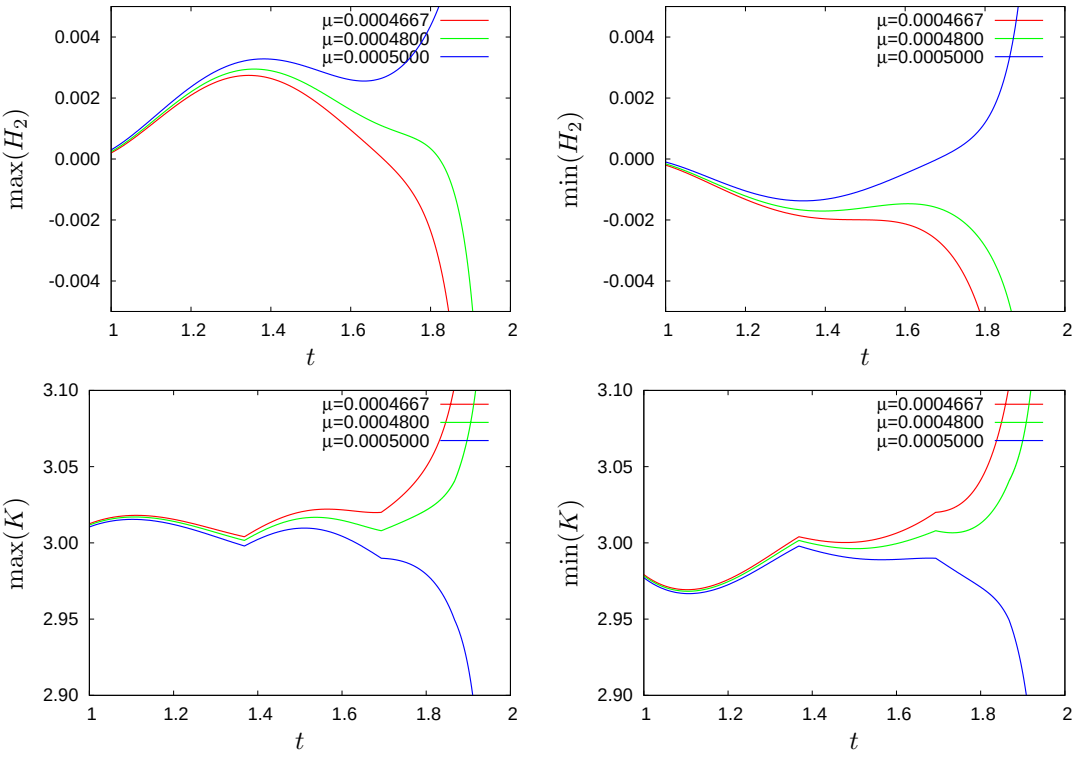

Fig. 4: Spatial minimum and maximum of H_2 and the Kretschmann scalar K vs. time

one choice of resolution parameters, i.e. we will not discuss convergence. However as far as we are able to check in practice, all the numerical errors in the results are convergent within the limits given by round-off errors which we only have limited control of.

Now we present our numerical results. Consider Fig. 4, where we show the following. On the horizontal axes, we plot the time coordinate t; recall that the initial hypersurface corresponds to $t = 1$ and that $t = 2$ would correspond to $\mathcal{J}^+$ if it exists. Hence, these plots show the future time evolution of the initial data chosen above. The past evolution will be considered below. On the vertical axis, for instance in the first of the four plots, we show the maximum value of H_2 at any given time t. In the early phase of the evolution, the solution behaves, as we would have expected from the spatially homogeneous case. Basically, the expansion of the coordinate $\mathbb{S}^2$-factor given by H_2 becomes more and more positive where it is positive initially, namely in particular at the maximum value at the poles of the sphere, see again Fig. 3. Furthermore, it becomes more and more negative where it is negative initially, namely at the minimum value at the equator of $\mathbb{S}^2$. This is the case for the evolutions of all the three initial data sets. Note also that the spatial profiles for H_2 are roughly unchanged qualitatively within this early epoch. However, after a short time $t \approx 1.3$, the behavior changes completely. In fact, the spatial profiles of H_2 start to become flatter again which can be seen in the figure by the fact that the maximal value of H_2 becomes smaller and the minimum value larger with increasing t.

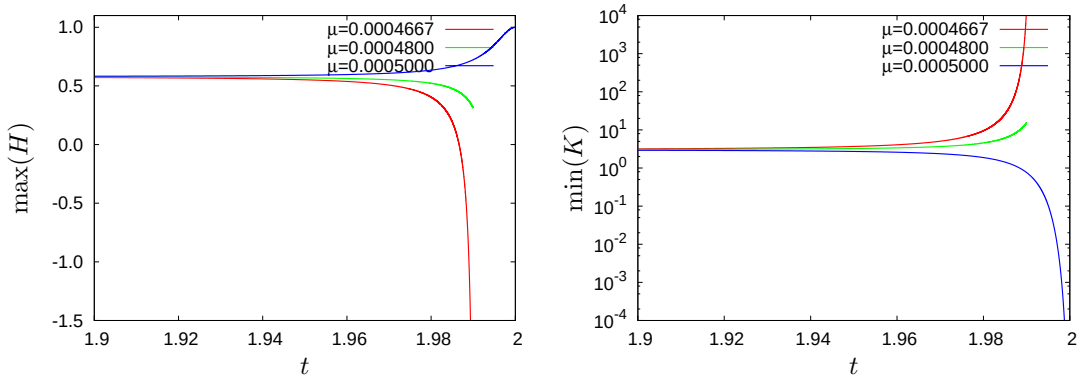

Fig. 5: The future behavior of the solutions for late times

Eventually the solutions make a decision whether the coordinate $\mathbb{S}^2$-factor expands or collapses indefinitely globally in space. We will show plots where the late time behavior becomes clearer in a moment. We do not understand the mechanism underlying this phenomena yet, and are only able to give a few more comments below. It is possible, that by means of the linearization of the problem, it is possible to explain, that in some way the "spatially homogeneous mode", which is small compared to the first "spatially inhomogeneous mode" initially, eventually dominates. This is currently work in progress. In any case, it seems obvious that there is a new instability built into the problem, in addition to the instability of the Nariai solutions which we were able to describe in the spatially homogeneous case before. Our choices of values of μ must be close to a critical value $\mu_c \in]0.00048, 0.0005[$. For $\mu < \mu_c$, the solution collapses eventually and for $\mu > \mu_c$ the solution expands eventually. It was a naive, and obviously false guess that this value is given by $\mu_c = 0.0004667$, i.e. our first choice of initial data, because in that case the initial curve of H_2 is completely symmetric with respect to the critical value in the spatially homogeneous case $H_2 = 0$. The fact that μ_c has a different value is a hint that there is an interesting new phenomenon underlying this instability.

In any case, consider also the similar plots for the Kretschmann scalar in Fig. 4. The curves are consistent with what we have just said. After the early time evolution, which is consistent with our expectations, the solution eventually makes a decision whether to expand or collapse globally. The kinks in these curves can be explained by the fact that the spatial profiles of the Kretschmann scalar are more complicated than those of H_2. In fact, several local extrema in space compete to become the global extremum. Note that this is not an important issue in the earliest stage of the evolution.

Let us look at Fig. 5 in order to check if our discussion so far is consistent with the late time future behavior of the solutions. In these plots, we again show the coordinate time t on the vertical axis, but this time only a small neighborhood of the final times where the runs were stopped. We do not need to show separate plots for maximum and minimum values here since in this situation their difference is hardly visible. In the first picture we show the Hubble scalar H, cf. Eqs. (12). In the eventually expanding case,

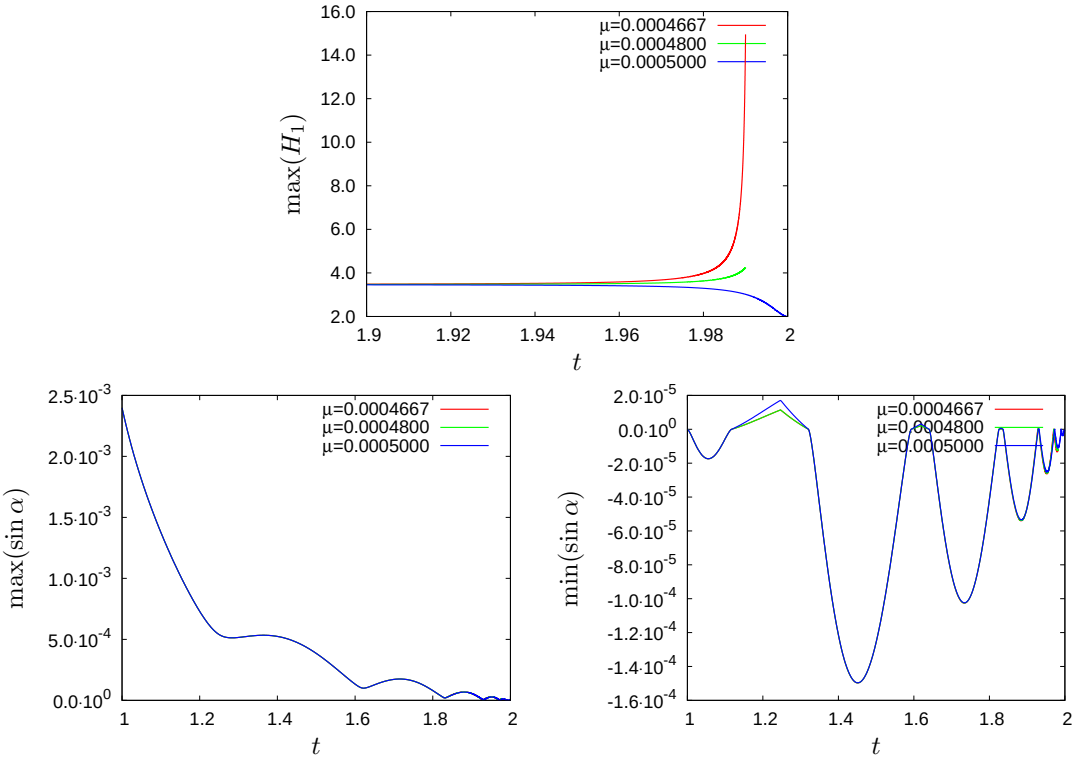

Fig. 6: Future behavior of the $\mathbb{S}^1$-factor and the angle between the $\mathbb{S}^1$- and the normal of the $\mathbb{S}^2$-factor.

given by $\mu = 0.0005$, its value reaches $H = 1$, which is the value consistent with the existence of a smooth $\mathcal{J}^+$. Indeed, we are able to compute the solution including $\mathcal{J}^+$, and hence provide evidence that this solution actually forms a smooth compact future conformal boundary. For the other two cases, which we refer to as the collapsing cases, our results suggest that they will collapse indefinitely. For the red case in the first plot in Fig. 5, this follows from a singularity theorem [1], since this plot demonstrates that H becomes smaller than -1. For the green case in the plot, we can at least show that the solution has the same tendency. There is no reason in principle that prevented us from continuing the numerical evolution underlying the green curve. However, we decided to stop both collapsing cases at $t = 1.99$, because these results already yield sufficient evidence for many of our conclusions. The second plot in Fig. 5 shows the minimum of the Kretschmann scalar K versus time t which supports our previous statements by blowing up for the collapsing evolutions and approaching zero for the expanding evolution.

Also, it is of interest to study the behavior of the other parts of the geometry. The first plot in Fig. 6 shows the evolution of H_1, cf. Eqs. (12), i.e. the expansion of the coordinate $\mathbb{S}^1$-factor. Recall that its geometry depends on the actual spatial point, and we have decided to plot the maximum value of H_1 here. We conjecture that the two collapsing evolutions form a singularity of cigar type [25] if H_1 blows up, as actually true

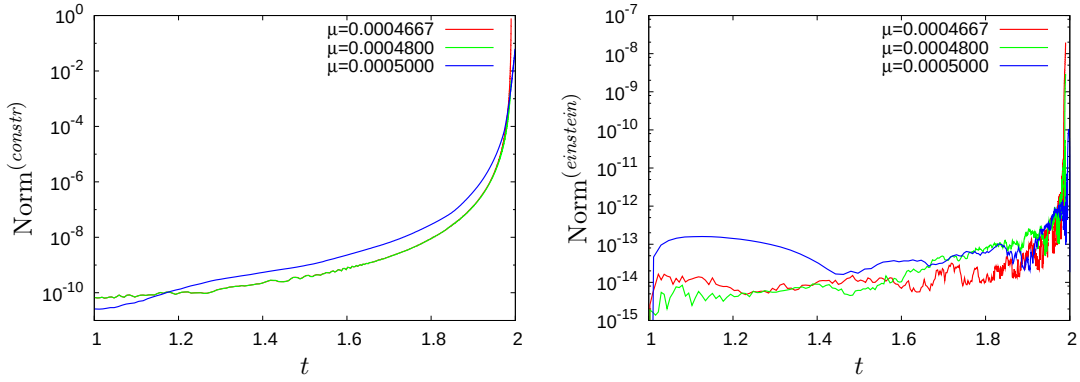

Fig. 7: Certain error norms vs. time

in the spatially homogeneous case. The next two plots in the figure show the maximum and minimum value of $\sin\alpha$, where at a given time $t = const$ and spatial point, the angle α is the angle between ∂_ρ and the normal vector of the coordinate $\mathbb{S}^2$-factor within the $t = const$-surface. We find that this angle approaches the value zero eventually, hence, loosely speaking, the Gowdy solutions become more and more polarized. Again, we do not understand the mechanisms underlying these curves, in particular why the polarized case seems to be an attractor and where these strange bounces come from. However, it turns out that the three curves are almost indistinguishable. So it is a natural question whether this behavior is universal in our class of solutions.

Before we make further comments on the question of instability of Nariai asymptotics, and also study the past evolutions, let us make some remarks concerning numerical errors here. We use the following definition of the norms of [4]. First, we define

$$\mathrm{Norm}^{(einstein)} := \left\| (\tilde{R}_{ij} - \lambda \tilde{g}_{ij})/\Omega(t) \right\|_{L^1(\Sigma_t)},$$

with the physical Ricci tensor $\tilde{R}_{ij}$ evaluated algebraically from the conformal Schouton tensor L_{ij} and derivatives of the conformal factor Ω. The spatial domain at time t is referred to as Σ_t here. The indices involved in this expression are defined with respect to the physical orthonormal frame given by $\tilde{e}_i = \Omega e_i$, and we sum over the L^1-norms of each component. Hence, this norm yields a measure of how well the numerical solution satisfies Einstein's field equations. Second, let us define $\mathrm{Norm}^{(constr)}$ as the L^1-norm of the sum of the absolute values of each of the six components of the left hand sides of Eqs. (17) at a given instant of time t. Now, consider Fig. 7. The violation of the constraints in the first plot appears quite bad, both in the collapsing case close to the singularity, which can be expected for evolutions in which the constraints are propagated freely in particular close to singularities, but also in the expanding case in a neighborhood of $\mathcal{J}^+$. In [4, 3], we saw similar problems with the evolution of the constraints. One explanation is that our formulation of the field equations, in particular, seems not to be optimal for constraint propagation. However, concerning our results here, there are hints that the situation is not as bad as it seems at first glance; certainly this has to

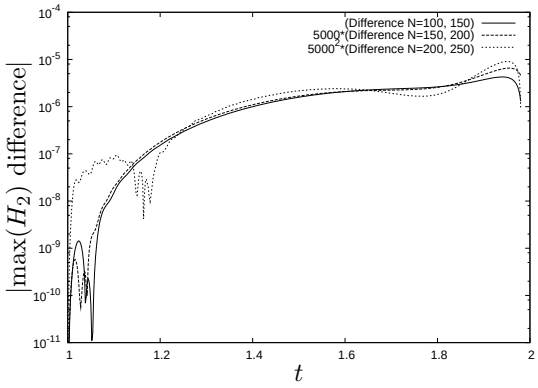

Fig. 8: Convergence of $\max(H_2)$ of spatial discretization for $h = 10^{-4}$, $\mu = 4.8 \cdot 10^{-4}$

be checked and improved in future research. First, the constraint violations in all three cases are of the same order of magnitude as when we compute the unperturbed Nariai solution with our formulation and numerical setup. When this numerical solution of the Nariai case is compared with the exact solution, it becomes clear that the absolute errors are much smaller than those expected from the constraint violations. That this situation might be the same for our runs here as well is actually suggested by the second plot showing $\mathrm{Norm}^{(einstein)}$. Another supporting argument is that the decision of the solutions whether to collapse or expand eventually takes place at very early times when the constraint violation is still very low.

Just as one example, we present a spatial convergence test in Fig. 8 for $\mu = 0.00048$. Similar tests have been performed in the other cases with the similar results. There are four runs underlying the figure for this one choice of initial data. In each of them, all adaption techniques have been switched off and the time step is always $h = 10^{-4}$. The first run is done with 100 spatial grid points, the second with 150, the third with 200 and the last with 250. In the plot, we show the maximum value of the modulus of the difference of the quantity H_2 between two successive runs versus time. Then these differences are multiplied with a factor which was chosen so that the three curves agree approximately. The result is that from intermediate evolution times on, the error determined by the spatial discretization is dominant and converges to zero with exponential convergence rate. At early times, the error is rather dominated by the time discretization and hence the three curves do not agree there.

Now let us proceed with the evolution in the past time direction. The unperturbed Nariai solution with $\sigma_0 < 0$ forms a Cauchy horizon there. What happens to this horizon under our perturbations? Consider the first plot of Fig. 9. Note that in the following plots, the initial hypersurface given by $t = 1$ is on the right of the plots and the past evolution takes place to the left. In this plot, we show the maximum of the Hubble scalar H for our three cases of initial data together with the corresponding curve of the unperturbed Nariai solution. Again, corresponding curves of the minima yield no further information. We see that the four curves in the plot are almost indistinguishable. Does

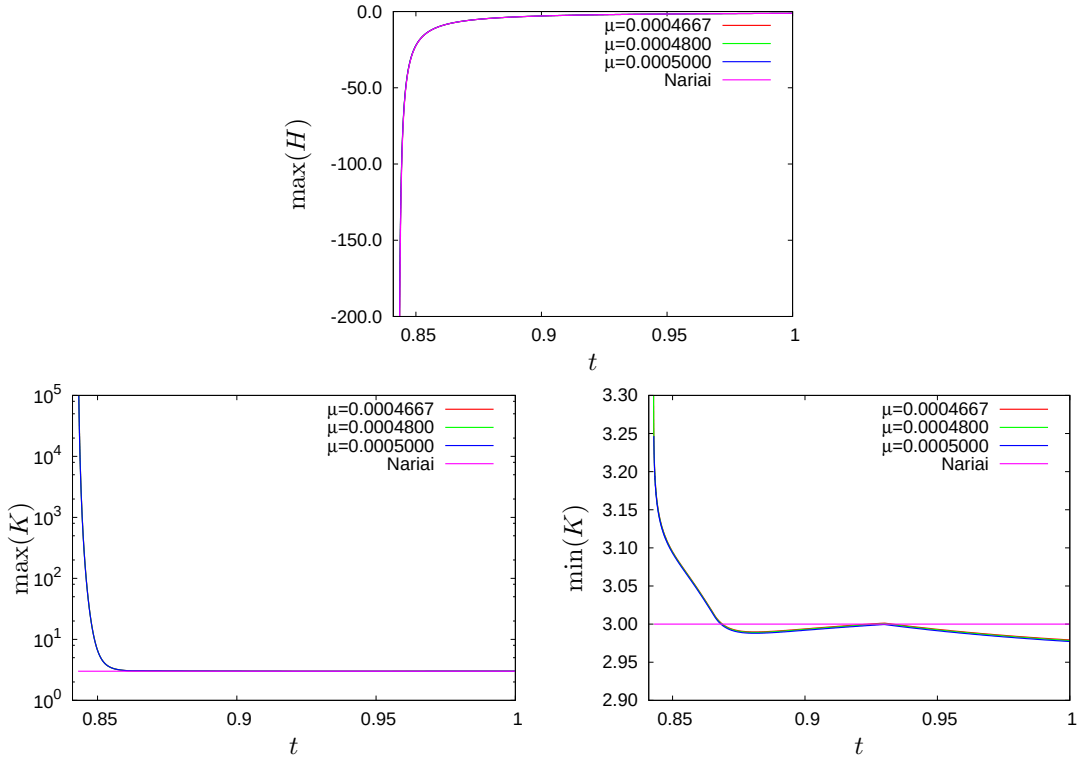

Fig. 9: Past evolution

this allow us to conclude about the existence of a Cauchy horizon even in the perturbed cases? The second and third plot in Fig. 9 suggest that this is not the case. Namely, for all perturbed solutions, the curvature blows up uniformly in the past. Certainly, the information obtained from the minimum of the Kretschmann scalar plotted in the third picture is not yet completely conclusive. However, it shows the right tendency. Possible reasons why the blow up of the minimum is so slow were discussed in the similar situation in [3], and one possible explanation is the choice of Gauss gauge.

8 Summary and outlook

In this paper we studied the question of instability of Nariai asymptotics for a family of inhomogeneous perturbations of certain generalized Nariai solutions. From our studies of the same question in the spatially homogeneous case in [5], our expectation for the instability of Nariai asymptotics in the inhomogeneous case was as follows. Under arbitrary small perturbations of the initial value of the expansion H_2 of the $\mathbb{S}^2$-factor of manifold, the $\mathbb{S}^2$-factor would expand exponentially and the solution would form a smooth conformal boundary at places where the initial value of H_2 is positive, and collapse to form a curvature singularity where the initial value of H_2 is negative. The outcome

would possibly be an arbitrarily complex multiple cosmological black hole spacetime, in accordance with the claims made in [6] for the spherically symmetric case.

However, our numerical results are different. The early time behavior is as expected. But then, the quantity H_2 starts to level off and the solution makes a decision, whether to either expand or collapse globally. We have presented the evolutions for three initial data. For one of them, the solution expands eventually in the future and even forms a smooth compact future conformal boundary, hence is consistent with the cosmic no-hair paradigm. In the other two case, we observe that the solution forms a curvature singularity in the future. In the past for all three cases, the Cauchy horizon of the unperturbed solution seems to be substituted by a curvature singularity, consistent with the strong cosmic censorship conjecture. In addition to the presentation here, we have also considered further choices of parameters and, if the initial amplitude of the inhomogeneity is not too large, the same qualitative behavior is found.

Due to our results, our picture has become more complicated than the naive picture obtained from the spatially homogeneous case. We are clearly able to confirm the instability of the asymptotics of the Nariai solution even in the spatially inhomogeneous Gowdy case. In contrast to our expectations, however, this instability is not local in space. Indeed the decision of the solution to either expand or collapse is global in space. This rules out the possibility to construct complicated multiple black hole solutions, in contrast to what is claimed in the spherically symmetric case. The underlying mechanism is not understood. It was particularly unexpected that our series of initial data enabled us to identify another instability; it is not the size of the initial perturbation of H_2 away from zero which plays the main role, but in some sense "how much H_2 is positive and how much it is negative". This is determined by our parameter μ. The values which we chose for μ in this presentation must be very close to the critical parameter. It would be interesting to determine the size of the critical parameter and explain its origin, but also to investigate if the critical solution – as for the other instability where the critical solution was a generalized Nariai solution – again has Nariai asymptotics in the sense that H_2 goes to zero in the limit $t \to 2$. Our numerical results here are not able to exclude this, cf. Fig. 4. We will study such outstanding and interesting questions in greater detail in future work. In particular, besides further numerical investigations, we have started to analyze the linearization of the field equation to complement our numerical results with some analytical insights. We cannot expect to understand the outstanding questions by such an approach completely. However, there is hope that some light would be shed on the problem of criticality here.

Our numerical results show no signs of spatially local behavior. In fact, the solutions seem to eventually expand or collapse globally in space. However, one can suspect that the spatial resolution, despite our spatial adaption technique, is too small and that local behavior is just smeared out. Of course, we cannot rule out this possibility. However, we believe that our adaption technique allows to monitor how much spatial resolution at a given time is actually needed and adapt the resolution according to the requirements. In any case, it is an unsolved problem why, in particular, we see no signs of Gowdy spikes in the collapsing cases. Possible resolutions of this problem were discussed in the

similar situation in [3]. One possible explanation is that, due our choice of Gauss gauge, the solution approaches the singularity in a too inhomogeneous manner, obscuring such small scale structure. This has to be investigated in future applications.

Certainly, our results have several limitations both technically and from our ansatz, some of which we list in the following. First, our class of initial data cannot be considered to be "generic", or put, the other way around, it is not clear how "special" it is. Thus it is hard to make any predictions about our questions for general solutions close to generalized Nariai solutions. We are currently working on a method to obtain arbitrary Gowdy symmetric solutions of the constraints in $\mathbb{S}^1 \times \mathbb{S}^2$ numerically. We will report on this in future work. But even with such techniques, it is not so obvious how to approach the general case systematically. As a first step, it would surely be interesting to study the polarized Gowdy case, i.e. to switch off the interesting behavior reported on above concerning the angle between the spatial $\mathbb{S}^1$- and $\mathbb{S}^2$-factor. It would be interesting to see how the dynamics is influenced by this qualitatively. Furthermore, this would also give us the chance to study our questions for generalized Nariai solutions with $\sigma_0 > 0$. A different limitation is that our technical infrastructure and our formulations still suffer from most of the problems listed in [4]; some of them were mentioned above. As one further example, we mention that investigations with such small inhomogeneities put strong demands on the numerical accuracy. As we reported in the similar situation in [3], our numerical infrastructure based on spectral methods is believed to be capable of this, at least up to a certain limit.

As another interesting related project, which we are currently working on, we have considered perturbations of Nariai solutions with very large inhomogeneous amplitudes. The hope is that the spatially local behavior, which was apparently suppressed in the case of small perturbations here, is present, and indeed we have found hints that this is the case. This will be reported on in another publication.

9 Acknowledgments

This work was supported by the Göran Gustafsson Foundation. Part of the work was done during the program "Geometry, Analysis, and General Relativity" at the Mittag-Leffler institute in Stockholm in fall 2008. I would like to thank in particular Helmut Friedrich and Hans Ringström for helpful discussions and explanations.

References

[1] L. Andersson and G.J. Galloway. dS/CFT and spacetime topology. *Adv. Theor. Math. Phys.*, 6:307–327, 2002, hep-th/0202161.

[2] F. Beyer. *Asymptotics and singularities in cosmological models with positive cosmological constant.* PhD thesis, Max Planck Institute for Gravitational Physics, Sep. 2007, gr-qc/0710.4297.

[3] F. Beyer. Investigations of solutions of Einstein's field equations close to λ-Taub-NUT. *Class. Quant. Grav.*, 25:235005, 2008, arXiv:0804.4224 [gr-qc].

[4] F. Beyer. A numerical approach for hyperbolic problems with spatial S3-topology. preprint, 2008, arXiv:0804.4222 [gr-qc].

[5] F. Beyer. On generalized Nariai solutions and their asymptotics. preprint, 2009, arXiv:0902.2531 [gr-qc].

[6] R. Bousso. *Adventures in de Sitter space*, pages 539–569. The future of theoretical Physics and Cosmology, Nov. 2003, hep-th/0205177.

[7] P.T. Chruściel. On space-times with $U(1) \times U(1)$ symmetric compact Cauchy surfaces. *Annals Phys.*, 202:100–150, 1990.

[8] A. Clausen and J. Isenberg. Areal foliation and AVTD behavior in T^2 symmetric spacetimes with positive cosmological constant. *J. Math. Phys.*, 48:082501, 2007, gr-qc/0701054.

[9] H. Friedrich. Einstein equations and conformal structure: Existence of anti-De Sitter-type spacetimes. *J. Geom. Phys.*, 17:125–184, 1995.

[10] H. Friedrich. *The Conformal Structure of Spacetime: Geometry, Analysis, Numerics*, chapter "Conformal Einstein Evolution". Lecture Notes in Physics. Springer, 2002.

[11] H. Friedrich and G. Nagy. The initial boundary value problem for Einstein's vacuum field equations. *Commun. Math. Phys.*, 201:619–655, 1999.

[12] D. Garfinkle. Numerical simulations of Gowdy spacetimes on $S^2 \times S^1 \times R$. *Phys. Rev. D*, 60(10):104010, Oct. 1999, gr-qc/9906019.

[13] R.H. Gowdy. Vacuum space-times with two parameter spacelike isometry groups and compact invariant hypersurfaces: Topologies and boundary conditions. *Ann. Phys.*, 83:203–241, 1974.

[14] S.W. Hawking and I.L. Moss. Supercooled phase transitions in the very early universe. *Phys. Lett. B*, 110(1):35–38, 1982.

[15] Intel. Intel Fortran Compiler, http://www.intel.com/support/performancetools/.

[16] J. Isenberg and V. Moncrief. Asymptotic behavior of the gravitational field and the nature of singularities in Gowdy space-times. *Ann. Phys.*, 199:84–122, 1990.

[17] H. Nariai. *Sci. Re. Tohoku Univ. Ser. 1*, 34(3):160, 1950.

[18] H. Nariai. On a new cosmological solution of Einstein's field equations of gravitation. *General Relativity and Gravitation*, 31(6), 1999.

[19] W.H. Press, S.A. Teukolsky, W.T. Vetterlin, and B.P. Flannery. *Numerical Recipes in C*. Cambridge University Press, 2nd edition, 1999.

[20] H. Ringström. Future stability of the Einstein-non-linear scalar field system. *Invent. math.*, 173:123–208, 2008.

[21] A.G. Sanchez and C.M. Baugh. Cosmological parameters 2006. preprint, 2006, astro-ph/0612743.

[22] D. N. Spergel et al. Three-year Wilkinson Microwave Anisotropy Probe (WMAP) observations: Implications for cosmology. *Astroph. J. Suppl. S.*, 170(2):377–408, 2007, astro-ph/0603449.

[23] F. Ståhl. Fuchsian analysis of $S^2 \times S^1$ and S^3 Gowdy spacetimes. *Class. Quant. Grav.*, 19:4483–4504, 2002, gr-qc/0109011.

[24] C. Stanciulescu. Spherically symmetric solutions of the vacuum Einstein field equations with positive cosmological constant. Master's thesis, University of Vienna, 1998.

[25] J. Wainwright and G.F.R. Ellis. *Dynamical Systems in Cosmology*. Cambridge University Press, 1997.